MOTION OF AIR BUBBLES IN STAGNANT WATER CONDITION

U. Bezdegümeli[1], O. Yeşin [2], S. Özdemir [1]

1: Department of Nuclear Safety, Turkish Atomic Energy Authority, Ankara, Turkey
2: Department of Mechanical Engineering, Middle East Technical University, Ankara, Turkey

Introduction

Bubbly two-phase flows appear in many industrial facilities such as nuclear power plants and chemical reactors. Especially in a boiling water type nuclear power reactor, bubbly flow characteristics affect the coolant circulation rate and consequently the other important reactor parameters. Therefore, in order to reach the desired level of safety and to obtain high operating efficiency at those facilities, understanding of the bubbly flows is important.

The behaviour of a single bubble is regarded as one of the basic elements characterizing the bubbly flow. So, analysis of single bubbles is very useful to understand basic flow mechanisms and to make the phenomenon of bubbly flow clear. On the other hand, it is very complicated to perform fully satisfactory theoretical analyses of the subject due to internal circulation of the bubble, shape deformation and oscillations causing bubble geometry change, secondary motion resulting in non-linear bubble path, and irregular rotation causing projected area change. Although we may get some useful quantitative and qualitative information from theoretical models [1-6], it is usually not sufficient for many cases, especially for deformed bubbles. Then, it is necessary to conduct experimental studies to fully understand the issue and to obtain the necessary data. Hence, we mostly rely on the experimental studies.

Test Set-Up and Experiment Procedure

The design details of the test set-up are shown in Figure 1. Distilled water is used in the system. Air is supplied to the system from a tank that is connected to an air compressor. The stored air is given to the system by a regulator that adjusts the pressure in the air supply line. Afterwards, air is injected into the test section through the bubble injector after passing through a needle type valve used for the adjustment of the bubble generation frequency.

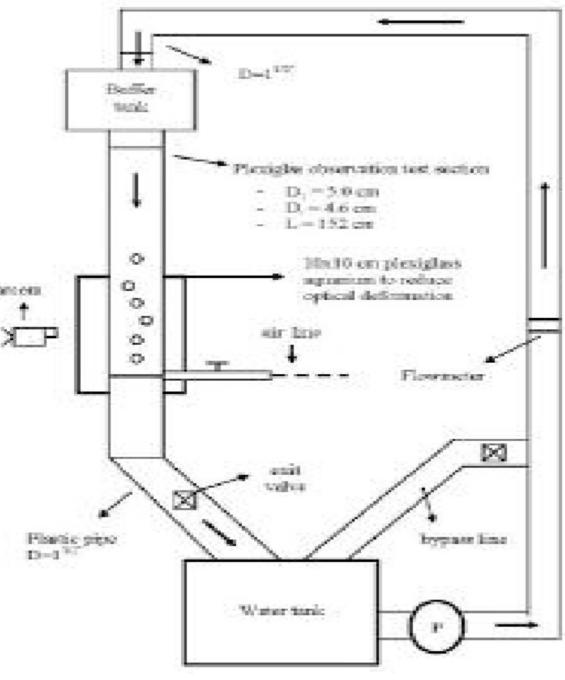

Fig 1. Test set-up

The main part of the test section is the cylindrical transparent plexiglas pipe enabling visualization of the bubble motion. To minimize optical deformations to a negligible level, a plexiglas aquarium was fixed onto the plexiglas pipe region where the camera shots were taken. Bubble injectors are cylindrical hollow brass pipes of 5.9 mm outer diameter drilled at seven different diameters (1.0-1.8 mm) to generate bubbles of different sizes. To be able to satisfy the negligible wall effect conditions ((d_b / D_h)≤0.12, [2]), the generated bubble diameters should be less than 5.5 mm. Bubbles, having diameters less than 4.2 mm, keep their spheroid shapes.

For greater diameters surface oscillations begin and bubbles get a rather irregular shape for diameters over 4.8 mm. Therefore, it has been decided not to investigate the bubbles having diameters greater than 4.8 mm. Since the maximum resolution the available image capture card (384x288 pixels) was not suitable, bubbles having diameters less than 3 mm were also not studied.

A monochrome camera with 1/5000 shutter speed was used for visualization of the experiments. Camera shots (25 frames/sec) were recorded in a computer hard disc by using a capture program and a capture card. Then, recorded video images were processed to analyze bubble motion and to obtain the data.

Results and Discussion

Bubble Path, Bubble Shape Behavior and Bubble Axial Relative Velocity Change

In the observed bubble diameter range, all bubbles move upward linearly for a few cm after being detached from the bubble injector surface, then show a planar zigzag motion similar to a sinusoidal shape. These observations are in good consistency with observations given in Refs. 5 and 8. According to Refs. 2 and 8, the cause of this secondary motion mode is wake shedding behind the moving bubble which occurs at Re_b higher than 200.

The shapes of the bubbles are almost prelate spheroid ($E \approx 1.18$) when they are mature and about to detach from the bubble injector surface [7]. Once they detach from the injector surface, the shape begins to be distorted due to the effect of the hydrodynamic pressure force, which increases with the increasing bubble velocity. The shape of the bubble becomes like a spherical cap and then oblate spheroid while following a linear path. Then, the bubble follows a zigzag path and begins to change its shape from sphere to disk with irregularly changing orientations or spherical cap. Careful examination of the recorded images showed that the magnitude of shape oscillations seems to be increasing with the increasing diameter.

Figure 2 shows the bubble relative velocity change in the vertical upward direction for three sample cases. Since the buoyancy force is much greater than the drag force, the bubble shows an accelerated motion with an increasing bubble velocity during the initial phase of the bubble motion after its detachment from the bubble injector. The increase in the bubble velocity and also the shape deformation cause an increase in the drag force, hence the magnitude of the bubble acceleration decreases until it reaches a maximum velocity. The decrease in the slope seen for the initial phase of the bubble motion is the result of this decrease in the acceleration. Thus, the experimental results are in good agreement with the theoretical expectations.

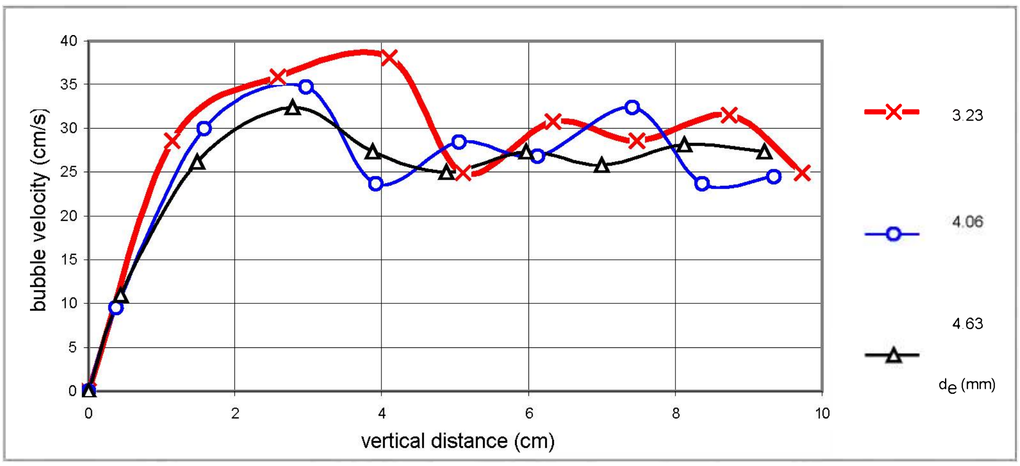

Fig 2. Bubble relative velocity change with the vertical distance

The bubble velocity drops to a certain value after passing a maximum, and then starts to oscillate within a band of 25-30 cm/s. The slope of this band is small and also decreases slightly with the increasing vertical travel distance.

The reason for this bubble velocity drop after passing through a maximum value is the change of bubble path from rectilinear to zigzag. While the bubble velocity vector had one component in the vertical direction during it is initial rectilinear motion, with the beginning of the zigzag motion the bubble velocity vector has two components; one in the vertical direction, the other in the horizontal direction.

Also, during the zigzag motion, the bubble shows irregular orientations and increased shape oscillations that may contribute to this bubble velocity decrease. The results are consistent with Ref. 5, which is unique in the literature.

Bubble Average Velocity and Drag Coefficient

The bubble velocity measurement technique used in this study is based on images recorded by a camera. The recordings were taken for the first 10 cm distance from the inlet due to the optimization of accuracies for the bubble velocity and bubble diameter measurements, which are both of the same importance for the study. Ref. 5 concludes that the bubble terminal velocity values are approximately equal to the average values of the bubble velocities measured between the initial vertical distance 5 cm and 10 cm.

Figure 3 gives the bubble average velocity as a function of bubble diameter and compares the results with Refs. 5 and 10. Bubble velocity values of this study are the average values calculated from the test data corresponding to the bubble travel distance between 5 to 10 cm.

It is seen that the velocity decreases from the value, 30 cm/s, to the value, 27 cm/s, between the bubble diameter range 3 mm to 4.2 mm and then this decrease becomes very slight for the rest of the bubble diameter range.

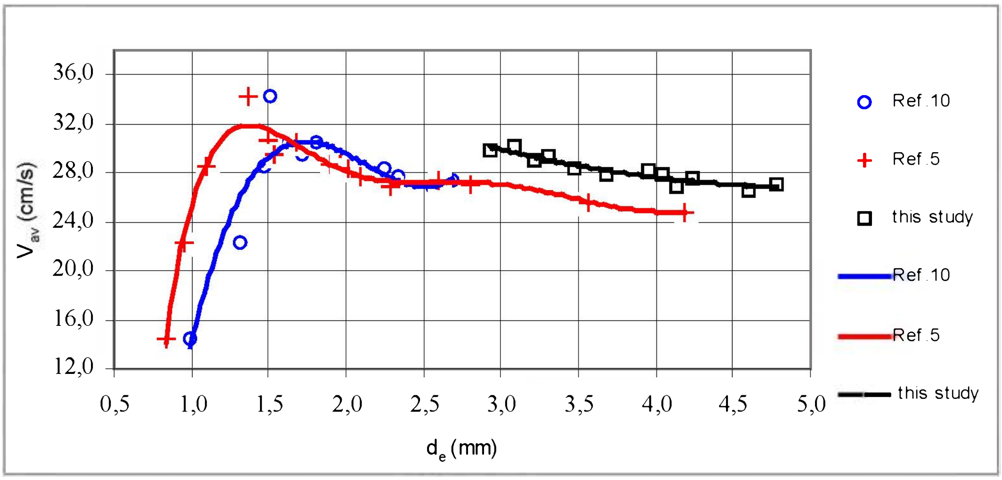

Fig 3. The bubble average relative velocity change as a function of equivalent bubble diameter

According to Refs. 2, 5 and 6, the rate of the bubble shape change (characterized by *E*) is decreasing with the increasing bubble diameter, and the aspect ratio, *E*, decreases more rapidly for smaller diameters.

Therefore, while the buoyancy force, having positive contribution to the bubble velocity, is increasing with the bubble diameter in the range of 3 mm to 4.2 mm, the drag force is also increasing more rapidly due to relatively rapid bubble deformation. As the rate of deformation decreases for d_e>4.2 mm, the rate of drag force increase nearly balances the rate of buoyancy force increase. This velocity behavior observed in the experiments shows a good consistency with the data found in Refs. 2, 5, 6, 8, 9, and 10. For a certain bubble diameter, the bubble average relative velocity values of this is 1.5-3 cm/s higher than the ones given in these references.

Figures 4 and 5 show the drag coefficient data of this study and compare the results with results of Refs. 5 and 10. As it is seen from Figure 4, $C_{D,av}$ increases with the increasing diameter. This is a consequence of bubble deformation, which also increases with the diameter.

Similar $C_{D,av}$ behavior is seen in Figure 5 which shows the change of $C_{D,av}$ as a function of Re_b. Since Re_b gives the ratio of the pressure forces to viscous forces and viscous effects are negligible for this range of bubble diameter, the main contribution to drag force comes from the pressure drag (form drag) component. Because of that reason, the level of the bubble deformation is important for the drag force.

If it is considered that the bubble velocities are approximately constant for the investigated range of bubble diameter (Fig. 3), from the bubble Reynolds number formula, $Re_b = \rho_l U d_e/\alpha_l$, it can be assumed that Re_b is only dependent on the bubble diameter and is a linear function of the bubble diameter as seen from the formula. Therefore, $C_{D,av}$ behavior is very similar to the one seen in Figure 4.

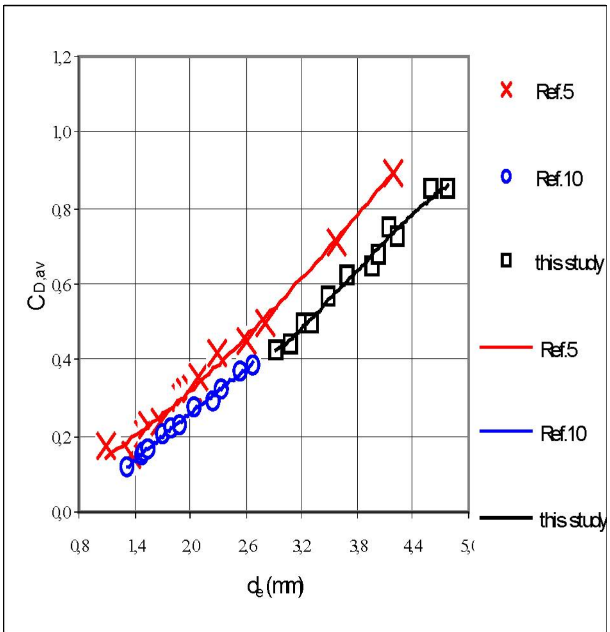

Fig 4. $C_{D,av}$ as a function of d_e

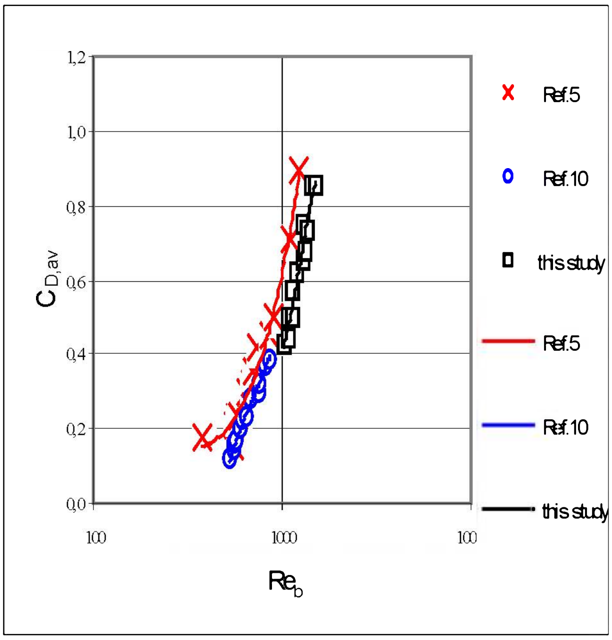

Fig 5. $C_{D,av}$ as a function of Re_b

Conclusions

For the studied range of diameters, all bubbles are accelerated to a maximum velocity in a rectilinear motion, then the velocity decreases and starts to oscillate in a slightly decreasing band with the bubble path changing from rectilinear to zigzag.

The bubble velocity decreases from 30 cm/s to 27 cm/s for the bubble diameter range of 3 mm to 4.2 mm and then this decrease becomes very small for larger bubble diameters, possibly due to the fact that the rate of drag force increase versus the rate of buoyancy force increase is nearly balanced as the rate of deformation decreases for d_e>4.2 mm. Drag coefficient values increase almost linearly with increasing bubble diameter or Re_b.

Nomenclature

$\mathbf{C_{D,av}}$	drag coefficient based on V_{av}	$\mathbf{Re_b}$	Reynolds number based on V_{av} and d_e
$\mathbf{d_b}$	bubble diameter, m	U	relative velocity of the bubble, m/s
$\mathbf{d_e}$	equivalent bubble diameter, m	$\mathbf{V_{av}}$	bubble average velocity between the distance 5-10 cm, m/s
$\mathbf{D_h}$	hydraulic diameter, m	μ_l	dynamic (absolute) viscosity of the surrounding liquid, kg/m.s
L	plexiglas pipe length from the bubble injection point	ρ_l	liquid density, kg/m^3

References

1. J.F. Harper, Adv. Appl. Mech., 12, 59-129, 1972.
2. R. Clift, J.R. Grace and M.E. Weber, “Bubbles, Drops and Particles”, Academic Press, New York, 1978.
3. P.C. Duineveld, J. Fluid Mech., 292, 325-336, 1995.
4. S.S. Sadhal, P.S. Ayyaswamy, and J.N. Chung, “Transport Phenomena with Drops and Bubbles”, Mechanical Engineering Series, Springer, 1997.
5. Altan Tapucu, “Durgun Sıvılar İçinde Yükselen Gaz Habbelerinin Hareketlerinin Etüdü”, Ph.D. Thesis, ITU, 1968.
6. A.W.G. de Vries, “Path and Wake of a Rising Bubble”, Ph.D. Thesis, Twente University, Netherlands, 2001.
7. Uğur Bezdegümeli, “Investigation of Air Bubble Motion in Counter-Current Water Flow Conditions”, Ph.D. Thesis, METU, Department of Mechanical Engineering, 2003.
8. I. Zun and J. Groselj, Nuc. Eng. and Design, 163, 99-115, 1996.
9. S.S. Sami, Nuclear Technology, 60, 124-136, 1983.
10. H. Yavuz, “Tabii Sirkulasyonlu Kaynar Sulu Reaktörlerde Buhar Habbelerinin Aşağı Sürüklenmesinin Etüdü, Ph.D. Thesis, ITU- Faculty of Machinery, 1970.